Anal Bioanal Chem (2013) 405:9071–9084
DOI 10.1007/s00216-013-7328-9

RESEARCH PAPER

Identification and characterization of individual airborne volcanic ash particles by Raman microspectroscopy

Natalia P. Ivleva · Susanne Huckele · Bernadett Weinzierl · Reinhard Niessner · Christoph Haisch · Thomas Baumann

Received: 16 May 2013 / Revised: 31 July 2013 / Accepted: 28 August 2013 / Published online: 13 October 2013
© Springer-Verlag Berlin Heidelberg 2013

Abstract We present for the first time the Raman microspectroscopic identification and characterization of individual airborne volcanic ash (VA) particles. The particles were collected in April/May 2010 during research aircraft flights, which were performed by Deutsches Zentrum für Luft- und Raumfahrt in the airspace near the Eyjafjallajökull volcano eruption and over Europe (between Iceland and Southern Germany). In addition, aerosol particles were sampled by an Electrical Low Pressure Impactor in Munich, Germany. As references for the Raman analysis, we used the spectra of VA collected at the ground near the place of eruption, of mineral basaltic rock, and of different minerals from a database. We found significant differences in the spectra of VA and other aerosol particles (e.g., soot, nitrates, sulfates, and clay minerals), which allowed us to identify VA among other atmospheric particulate matter. Furthermore, while the airborne VA shows a characteristic Raman pattern (with broad band from ca. 200 to ca. 700 cm^{-1} typical for SiO_2 glasses and additional bands of ferric minerals), the differences between the spectra of aged and fresh particles were observed, suggesting differences in their chemical composition and/or structure. We also analyzed similarities between Eyjafjallajökull VA particles collected at different sampling sites and compared the particles with a large variety of glassy and crystalline minerals. This was done by applying cluster analysis, in order to get information on the composition and structure of volcanic ash.

Keywords Individual airborne particles · Volcano · Eyjafjallajökull · Raman microspectroscopy (RM) · Identification · Characterization

Introduction

During the eruption of the volcano Eyjafjallajökull in Iceland (63.63° N, 19.62° W, 1,666 m a.s.l) in April/May 2010 volcanic ash (VA) plumes were ejected into the atmosphere to over 9 km a.s.l [1–3]. The volcano belched 10 (2.5–50) Tg of distal ash mass and about 3 (0.6–23) Tg of SO_2 over the whole eruption period [4]. The VA was dispersed all over Europe and, as a consequence, air traffic ceased in 23 European countries; 75 % of the European airport network was closed, with more than 100,000 flights cancelled, which affected 10 million passenger journeys between April 14 and April 20 (as reported by EUROCONTROL, from [4]). Further incursions of VA over Western Europe caused again airspace closures at various places and periods until May 18, 2010, leading to the cancellation of about 7,000 more flights. It was first time ever when a volcanic eruption critically impacted such a large and busy air space [4].

Several studies on the characterization of Eyjafjallajökull VA, including airborne particles, were performed during the last 3 years [1–8]. Gislason et al. have collected a set of dry ash samples immediately after the explosive event (April 14, 2010) and compared with fresh ash from a later, more typical eruption using electron microprobe (EMPA), scanning electron microscopy (SEM), X-ray diffraction (XRD), atomic force microscopy, and inductively coupled plasma optical emission spectroscopy [2]. During the time period of the Eyjafjallajökull eruption (April/May 2010), the Düsseldorf

Electronic supplementary material The online version of this article (doi:10.1007/s00216-013-7328-9) contains supplementary material, which is available to authorized users.

N. P. Ivleva (✉) · S. Huckele · R. Niessner · C. Haisch · T. Baumann
Institute of Hydrochemistry, Chair for Analytical Chemistry, Technische Universität München, Marchioninistr. 17, Munich 81377, Germany
e-mail: Natalia.Ivleva@ch.tum.de

B. Weinzierl
Deutsches Zentrum für Luft- und Raumfahrt (DLR), Institut für Physik der Atmosphäre, Oberpfaffenhofen 82234, Germany

University of Applied Sciences has performed several research flights over Germany. In parallel, the measurement flights have been performed by the University of Iceland in May 2010 over the western part of Iceland. For the measurement flights, aircrafts were equipped with optical particle counters for in situ measurements. Additionally, the airborne particles were analyzed by SEM equipped with an energy dispersive X-ray spectrometer (EDX) and XRD [8]. In order to provide information on the ash plume in many perspectives (in particular on the particle properties, spatial distribution, horizontal and vertical depth), the DLR Falcon research aircraft performed 17 flights in VA plumes over Europe between Southern Germany and Iceland during the major eruption period of the Eyjafjallajökull volcano in April/May 2010 [4]. This aircraft is equipped with a LIDAR (light detection and ranging) backscatter, instruments for particle number-size distribution and absorption measurements and further trace gas and meteorological instrumentation. Sampled airborne VA particles were characterized using SEM/EDX and transmission electron microscopy (TEM) [4, 5].

Although different methods for the analysis of chemical composition and structure of VA have been already applied [2, 4, 8], to the best of our knowledge, no work concerning the identification or characterization of individual airborne VA particles from Eyjafjallajökull (or generally from volcanoes) using Raman microspectroscopy (RM) has been published so far. RM, which is based on the effect of an inelastic light scattering by molecules, provides fingerprint spectra and allows the non-destructive distinction of a wide range of chemical substances in air particulate matter with the spatial resolution of an optical microscope [9, 10]. Regarding the VA particles, RM can help not only in the characterization of their mineral composition with the spatial resolution down to several microns but also in the determination of crystalline (ordered and disordered) or glassy (amorphous) structure of volcanic ash. Moreover, the future analysis (e.g., by applying of Raman mapping together with cluster analysis) of large number of particles from an ash plume may give an insight in the total fraction of VA particles in the aerosol. This information can be useful for the correct prediction of absorption properties of ash clouds and for the accurate determination of ash concentration in plumes. Furthermore, the detailed knowledge of chemical composition and structure (crystalline and/or glassy) of VA particles can help to answer the questions about the danger of ash particles for aircrafts and the VA impact on public health and environment.

In order to assess potential damage for jet engines, one has to know not only the total mass of particles and their size distribution but also their mineralogical composition (glassy particles, crystalline particles) and their oxidation state (amorphous iron oxides vs. eg. hematite). For instance, dust from the Sahara is less problematic compared to volcanic ash [11].

This paper summarizes results of Raman microspectroscopic analysis of individual airborne VA particles collected in April/May 2010 during the DLR research aircraft flights in the airspace near the eruption and over Europe (between Iceland and Southern Germany) [4] as well as of the aerosol sampled with an Electrical Low Pressure Impactor (ELPI) in Munich, Germany. The presented results not only demonstrate for the potential of RM for the identification and chemical characterization of single VA particles but also provide the basis for more detailed RM studies of airborne VA.

Experimental

Samples of fresh and aged airborne VA particles suitable for single particle RM analysis were collected on Particle Soot Absorption Photometer (PSAP) filters by sampling device inside the cabin downstream of the Falcon aerosol inlet on May 2 (flight from Keflavik to Stornoway with the measurements in the top part of the fresh plume over the North Atlantic) and May 18 (aged ash plume survey over Germany and North Sea, German air space closure was under consideration), respectively (see Schumann et al. [4] for more details). On May 18, the plume reached Southern Germany and the Alps and almost over the entire Falcon flight, multiple VA layers were observed over Germany by the LIDAR. The PSAP filter samples (especially from aged ash plume) contain not only VA but also common atmospheric aerosol particles such as soot. In addition, aerosol samples collected from April 16 until April 19 at ground level in an urban setting at the Institute of Hydrochemistry, Chair for Analytical Chemistry, Technische Universität München (48.15°N, 11.58° W, 527 m a.s.l) using an ELPI (Model EFS1 90 Nr. 90114, Dekati Ltd., Tampere, Finland; ELPI 2003) were analyzed. The VA particles sampled with ELPI may originate from the ash plumes ejected into atmosphere during the Eyjafjallajökull eruption on April 14, 2010 and dispersed than over Europe. According to the LIDAR system observations over Munich reported by Gasteiger et al. [6] the first traces of ash were detected in the evening on April 16, and the maximum of the ash layer was observed in the morning on April 17. No aerosol sampling at the ground level in May 2010 was done due to technical difficulties with the ELPI system. Additionally, volcanic ash particles taken at ground near the eruption (June 2010) were studied. An overview of the samples which were analyzed by RM is shown in Table 1.

Raman spectra of all samples were recorded by a Horiba LabRAM HR Raman microscope system (Horiba Jobin Yvon, Japan) using an excitation wavelength λ_0 of 633 nm (He–Ne laser, 35 mW initial intensity, ca. 14 mW at the sample). Calibration was accomplished by the characteristic first-order phonon band of Si at 520.7 cm^{-1} from a silicon wafer and zero order correction of a blazed grating with a groove density of 600 lines mm^{-1}. Spectra were collected in the Stokes shift range from 50 to 2,000 cm^{-1} with a ×100

Table 1 Overview of the representative samples analyzed by RM

Samples	Sampling details	Date	Filter/substrate	Particle size[a] (μm)
VA-fp 1–5	DLR Falcon flight near the Eyjafjallajökull volcano eruption [4], airborne, fresh plumes (fp)	02.May.2010	PSAP filter	2–50
VA-ap 1–4 ap 5–7	DLR Falcon flight over Germany and North Sea [4], airborne, aged plumes (ap)	18.May.2010	PSAP filter	2–10
ELPI 1–6	Test field in Munich, ELPI samples collected near the ground, airborne	16.April–19.April.2010	Al foil	2–3
VA-g 1–9	Samples taken at the ground (g) near the Eyjafjallajökull volcano	June 2010	–	50–200

[a] Size of particles measured by RM

magnification objective (NA=0.9), confocal hole diameter 100 μm, that corresponds to lateral and axial resolution of ca. 1 and 2 μm, respectively. The RM analysis of more than 140 single particles was performed directly on PSAP filters or on Al foil substrates used for sampling by the Falcon and the ELPI, respectively. No noteworthy Raman signals were detected for both substrates. Laser intensity was decreased to 1 % of initial intensity (i.e., 0.14 mW at the sample) to avoid the damage of VA particles due to heating. Integration time for one spectrum was set to 10 s, and the number of accumulations from 10 to 20 was adjusted in order to obtain an acceptable signal-to-noise ratio. The Raman spectra were baseline corrected, normalized, and shifted in the Figures for better visualization. The unprocessed spectra are shown in the Electronic supplementary material (ESM; Fig. S1–S6). For the analysis, particle size and morphology, the pattern in Raman spectrum (revealing mineral composition and structure), and the particle stability with respect to the intense laser beam were taken into account. The mineral basaltic rock (Mineral collection of TUM, Chair of Engineering Geology) was also analyzed by RM, and its spectra were used as references, together with the spectra from the database SpecID, Horiba Scientific, i.e. quartz group minerals (quartz SiO_2, tridymite SiO_2); amorphous silicon oxide of natural (glass mineral obsidian SiO_2, mineraloid opal $SiO_2 \cdot nH_2O$) and synthetic origin (suprasil SiO_2); alkali feldspars (microcline $KAlSi_3O_8$, orthoclase $KAlSi_3O_8$, sanidine $(K,Na)(Al,Si)_4O_8$); plagioclase feldspars (albite $NaAlSi_3O_8$, anorthite $CaAl_2Si_2O_8$, oligoclase $(Na,Ca)(Al,Si)_4O_8$); plagioclase feldspar glasses (albite glass, anorthite glass); feldspathoid (silica-unsaturated aluminosilicate, i.e., nepheline $NaKAlSiO_4$); amphibole (actinolite $Ca_2(Mg,Fe)_5Si_8O_{22}(OH)_2$, amosite $(Mg,Fe)_7Si_8O_{22}(OH)_2$, anthophyllite $(Mg,Fe)_7Si_8O_{22}(OH)_2$, crocidolite $Na_2Fe_2Si_8O_{22}(OH)_2$, glaucophane $Na_2(Mg,Fe)_3Al_2Si_8O_{22}(OH)_2$, hexagonite $Ca_2(Mg,Fe)_5Si_8O_{22}(OH)_2$, hornbendene $Ca_2(Mg,Fe)_4AlSi_7AlO_{22}(OH)_2$, nephrite $Ca_2(Mg,Fe)Si_8O_{22}(OH)_2$, talc $Mg_3Si_4O_{10}(OH)_2$, tremolite $Ca_2(Mg,Fe)_5Si_8O_{22}(OH)_2$); pyroxene (aegirine $NaFeSi_2O_6$, augite $(Ca,Mg,Fe)_2Si_2O_6$, bronzite $(Mg,Fe)SiO_3$, clinoenstatite $MgSiO_3$, diopside $CaMgSi_2O_6$, enstatite $MgSiO_3$, hedenbergite $CaFeSi_2O_6$, jadeite $NaAlSi_2O_6$, kunzite/spodumene $LiAlSi_2O_6$); olivine (fayalite Fe_2SiO_4, forsterite Mg_2SiO_4, peridot $(Mg,Fe)_2SiO_4$); biotite $K(Mg,Fe)_3(Al,Fe)Si_3O_{10}(OH,F)_2$; ilmenite $FeTiO_3$; goethite (α-FeOOH); lepidocrocite (γ-FeOOH); limonite $(Fe_2O_3 \cdot nFeO \cdot nH_2O)$; hematite (α-$Fe_2O_3$); magnetite ($Fe_3O_4$); anatase ($TiO_2$); $NaNO_3$; $CaSO_4$; soot (carbon black).

Cluster analysis (CA) was performed using the software package R [12] and R packages cluster (http://cran.r-project.org/web/packages/cluster/index.html) and Peaks (http://cran.r-project.org/web/packages/Peaks/index.html). Spectra were imported into R and aligned to integer wavenumbers. Spectra from collected particles were fitted using a Gaussian fit with $\sigma=2$ for Raman shifts<=1,100 cm^{-1} and $\sigma=4$ for Raman shifts>1,100 cm^{-1} to account for the broader soot bands. The peak fitting procedure also removes the background [13–15]. Peaks with amplitude below 2 % of the maximum intensity were discarded and not used for further evaluation. Clusters were calculated for the background corrected and fitted Raman spectra in the spectral range between 100 and 1,650 cm^{-1}, using divisive hierarchical clustering based on Euclidian distances [16].

Results and discussion

Identification of VA particles

Figure 1 shows the optical microscope images of representative VA aerosol particles VA-fp 1–5 from fresh plumes collected during the DLR flight on May 2 near the eruption and the corresponding Raman spectra. The volcanic particles are brownish with a characteristic shape, like droplets solidifying by sudden cooling. The spectra are characterized by a very broad band which extends from ca. 200 to ca. 700 cm^{-1}. This band is typical for glassy structures, such as SiO_2 glasses, alumosilicate (basaltic and rhyolitic) glasses [17], feldspar glasses (see below), as well as natural volcanic glasses (phonolite glass from Canary Islands, obsidian glass from Iceland, and perlite from the Eastern Rhodopes) [18]. In addition, relatively broad peaks near 140, 310, 390, 415, 540, 720, and 860 cm^{-1} can be found in the spectra (Table 2). The latter peaks suggest the presence of different minerals (see

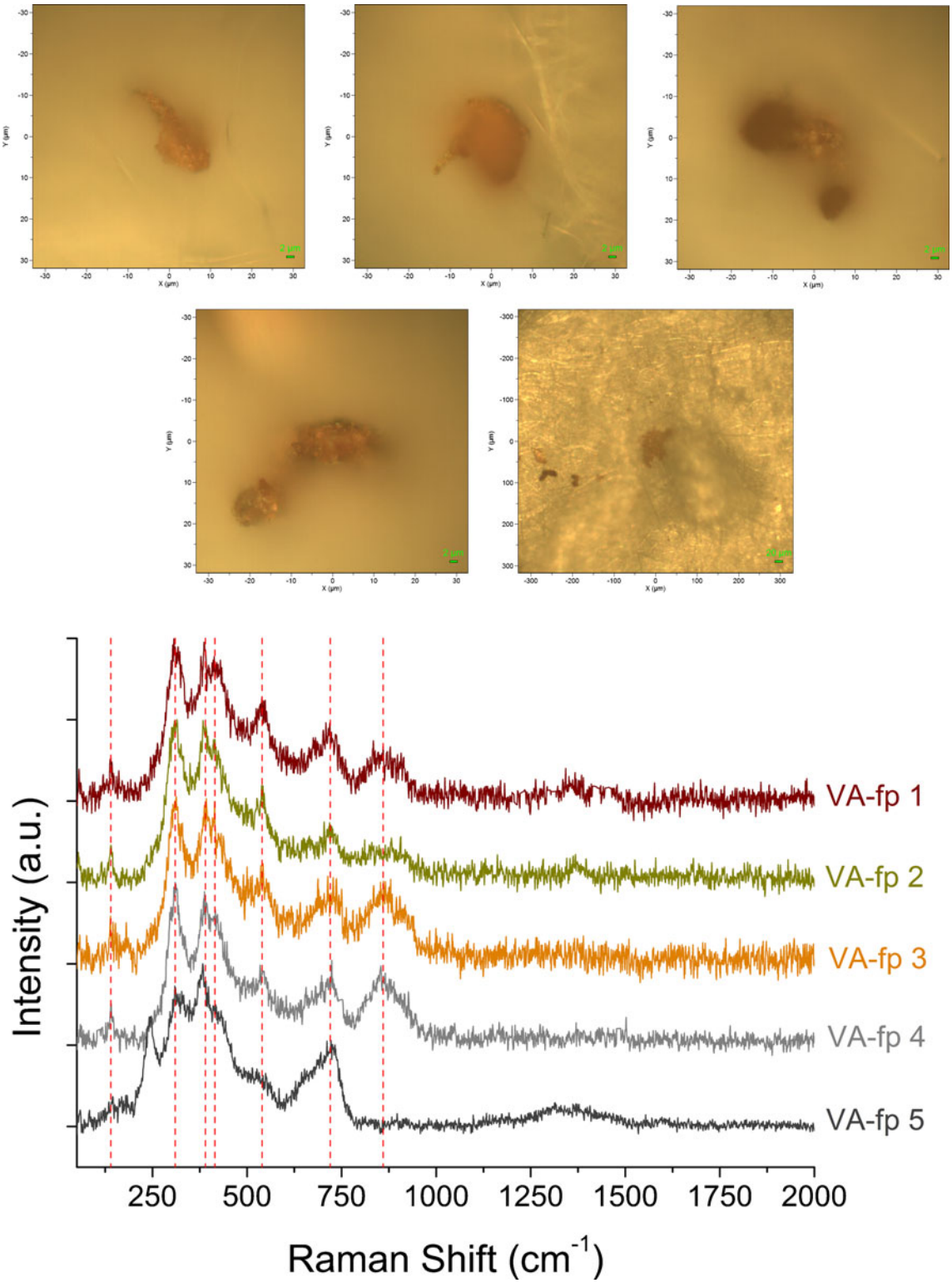

Fig. 1 Optical microscope images and corresponding Raman spectra of the airborne particles (VA-fp) collected in the atmosphere near the eruption of Eyjafjallajökull volcano on May 2, 2010 (fresh plume)

"Characterization of VA particles" section for more details) with rather disordered crystalline structure. It should be mentioned that significant changes in the VA-fp particle shape and color were observed if relative high laser power (14 mW at the sample) was applied (Fig. S7, ESM). Therefore, reduced (0.14 mW at the sample) source power was used for the analyses. Our finding regarding the behavior of VA particles is in agreement with Casadevall et al. [11], who pointed out that volcanic ash is considered more dangerous to air traffic, and aircraft engines in particular, than desert dust due to its lower melting temperature. We can assume a complex structure of VA-fp particles, where different crystalline mineral particles are embedded in glassy matrix. This assumption is in accordance with results of SEM analysis of airborne Eyjafjallajokull VA particles reported by Weber et al. [8], where crystals embedded in glassy matrix were found along with particles with typical glass and well-developed crystal structure. Also, Gislason et al. [2], who studied Eyafjallajökull volcanic ash (collected at the ground on April 15 and 27) by EMPA and XRD, demonstrated that particles are dominated by andesitic glass, which has a Mohs scale hardness of about 5.5–6. The Eyjafjallajökull glass softens at approximately 890 °C and melting is complete at 1,147 °C. Thus, the ash would easily melt in a jet engine, which reaches temperatures of 1,500–2,000 °C [2].

Figure 2 shows the optical microscope images of typical VA airborne particles VA-ap 1–4 and ap 5 from the aged plume (which includes not only VA, but also common atmospheric aerosol particles), collected during the DLR flight on May 18 over North Sea and Germany (including the airspace near Munich), and the corresponding Raman spectra. On average, the size of VA-ap (2–10 μm) is comparable or smaller than the one of VA-fp (2–50 μm). This finding is in agreement with the literature: Schumann et al. reported that particles collected at wing stations during the DLR flights had diameters up to 20 μm, with size- and age-dependent composition. The effective diameter from the particle size distribution was near 7 (4–10) μm for the fresh plume. The plumes of ages larger than 2 days were free of particles larger than 15 μm due to sedimentation, unless the particles were porous with significantly smaller effective density [4]. The shape of aged particles VA-ap 1 and VA-ap 3 looks similar to the particles VA-fp 1–4, collected in the airspace near the eruption. The comparison of their spectra reveals also the similarities in the characteristic spectral pattern, especially for the particles VA-ap 3 and VA-fp 5 (see below and Table 2). Vertical lines in Figs. 1 and 2 mark the characteristic bands of airborne particles VA-fp 1–5 and VA-ap 1–4. The differences between the spectra of VA collected on May 2 (VA-fp 1–5, Fig. 1) and May 18 (VA-ap 1–4, Fig. 2) suggest differences in their chemical composition and structure (e.g., due to variable proportions of

Table 2 Wavenumbers on Raman spectra of VA particles and reference compounds

VA particles	VA-fp	200–700m		140m	245[a]m	310s	390s	415s		540m,br			720m,br	860m,br
	VA-ap	200–700m	115[a]w	140[a]m,br	245[a]m	310s,br	390[a]s,br	415[a]m,br		540[a]m,br		670[a]vs	720m,br	860[a]s,br
	ELPI 1	200–800s		147w	225vs	293vs		410s			612s,br	660s,br		
	ELPI 2	200–800m		155m,br	224m	290m,br		415m,br			610s,br	690vs,br		
	ELPI 3	200–800s		185w,br			360s,br			500s,br		680s,br		
	VA-g		105[a]w,br	162m,br	215[a]s	285m,br			470s	511vs		660m,br		1,000[a]m,br
Reference compounds	Basalt 1, 3		128[a]m		226s, 246[a]w	293vs		410m,br	466m-s	510[a]m	612m,br	660m,br		
	Basalt 2-4		128m		205m,br, 265w		356vw		465vs					
	Quartz		128m		206m,br, 265w				465vs					
	Goethite				206w, 247m		300s, 386vs	418m	482w	550s		680w		
	Hematite				226vs, 246w	293vs		411s	498w		612w	680[a]m		
	Magnetite									532w,br		664vs,br		
	Microcline		127m	157m	200w, 266m	286m		455m	476ms	514vs			750m	813m, 844mw,br
	Albite			162ms	207m	288s		406w	477s	505vs				
	Oligoclase				208s	290s			480s	507vs				
	SiO_2 glass	200–700s							490s		605m,br			805m,br

[a] Bands found not for all VA particles of distinct sample type

vs very strong, *s* strong, *m* medium, *w* weak, *br* broad

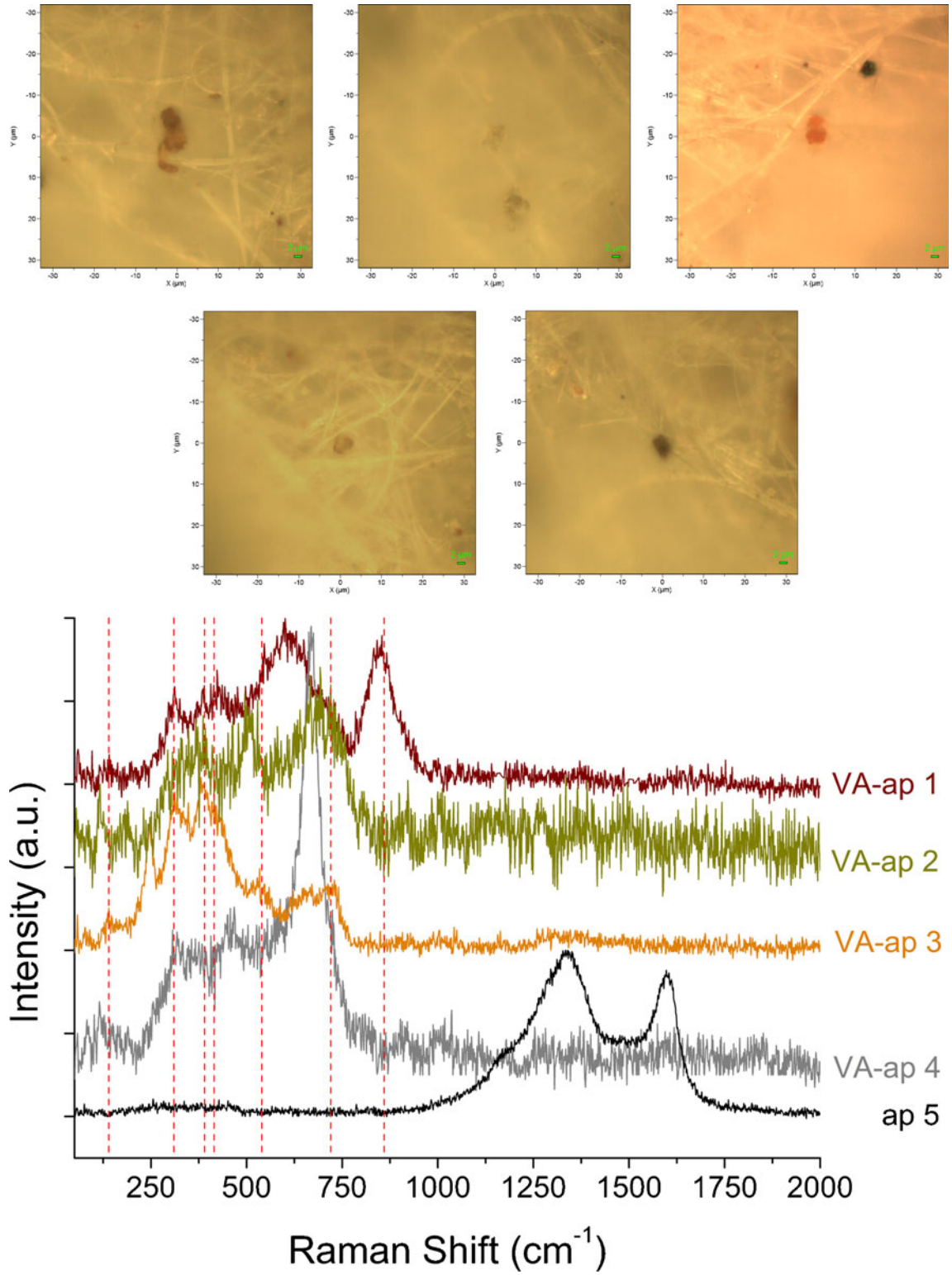

Fig. 2 Optical microscope images and corresponding Raman spectra of the airborne particles (VA-ap and ap) collected in the airspace over Germany and North Sea on May 18, 2010 (aged plume)

the different minerals, partial precipitation, and/or chemical aging during the transport) of the VA from aged plume compared to the fresh one. This finding is in good agreement with data on TEM and SEM analysis of VA [2, 4]. Schumann

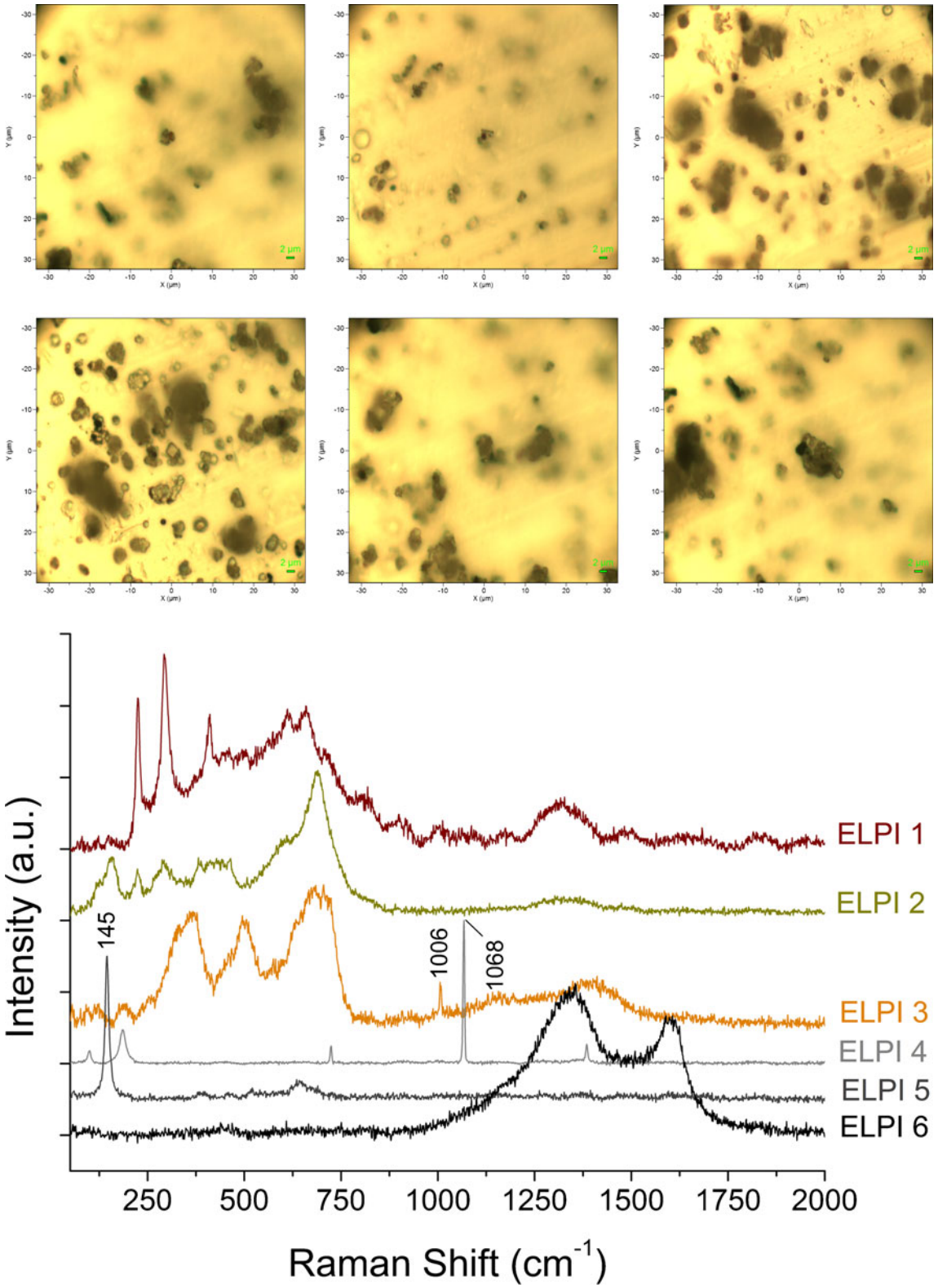

Fig. 3 Optical microscope images and corresponding Raman spectra of the aerosol particles (ELPI) collected with the ELPI, Munich from April 16 to 19, 2010. The spectra were collected at the positions $x=0$, $y=0$

et al. [4] found that silicates and mixed particles are the most abundant groups for the particles larger than 500 nm (below a size of 500 nm, the aerosol is dominated by secondary particles such as ammonium sulfates/nitrates). In the samples of

fresh and aged VA, most silicate grains (more than 90 %) are mixtures of various minerals. The composition of the silicates (external and within the mixtures) is different for the two sampling days. For example, the Si/Al atomic ratio decreases from 3.6±2.8 on May 2 to 2.8±1.2 on May 17, indicating an increasing feldspar component. The iron content is higher on May 2 with an atomic Fe/Si ratio of 0.33 compared to Fe/Si= 0.08 for May 17 [4].

Gislason et al. [2], who analyzed Eyafjallajökull volcanic ash (collected at the ground on April 27) before and after exposure to pure water and HNO_3 (90 min, 10^{-3} M), reported Fe/Si ratios 0.13 (untreated), 0.14 (H_2O-treated), and 0.051 (HNO_3-treated), indicating the decrease of iron content after the treatment with acid solution.

In the aged plume, we also found typical atmospheric aerosol particles, such as soot, with characteristic G (graphite) and D (defect) bands near 1,600 and 1,330 cm^{-1}, respectively (ap 5 in Fig. 2, as well as particles ap 6 and ap 7, not shown), in addition to volcanic ash.

We also analyzed aerosol samples collected from April 16 until April 19 at ground level in Munich, Germany, using an ELPI. The VA particles sampled with ELPI may originate from the volcanic plumes, which were ejected into atmosphere during the Eyjafjallajökull eruption on April 14, 2010 and reached Munich on April 16 (with a maximum concentration on 17 May), as observed via LIDAR by Gasteiger et al. [6].

The optical microscope images and the corresponding Raman spectra of the particles (ELPI 1–6) collected in Munich using ELPI are shown in Fig. 3. Although it was difficult to distinguish visually the VA particles from the typical atmospheric aerosol particles, which were also sampled on Al substrates, we were able to identify the VA particles according to their characteristic pattern in the Raman spectra below 1,000 cm^{-1}. The VA particles are smaller (2–3 μm) than to the particles collected during Falcon flights (up to 50 μm), look dark and rather crystalline. The ELPI 3 particle shows not only the broad bands below 1,000 cm^{-1} (Table 2) typical for VA but also the peak at 1,006 cm^{-1} which can be assigned to calcium sulfate. The formation of sulfates can be associated with the high amount of SO_2 in VA plumes. Schumann at al. [4] for instance found small ammonium sulfate particles, which crystallized from droplets onto the surface of mixed silicates particles. However, we cannot exclude the impact of SO_2 from urban-industrial atmosphere of Munich in aging of VA and particularly in formation of calcium sulfate on the surface of VA particles.

The differences in the particle size and the corresponding Raman spectra between of VA particles from fresh/aged plumes collected during Falcon flights (May 2010) and the VA particles collected at ground level in Munich by the ELPI (April 2010) can be explained not only by the aging of the particle during the transport but also by the different eruption events. Gislason et al. [2] pointed out that the explosive ash particles emitted during the Eyjafjallajökull eruption (beginning on April 14), which reached Europe in a jet stream, were especially sharp and abrasive over their entire size range from tens of nanometers to hundreds of micrometers. The authors sampled the particles on April 15 and 27 and found that the ash from April 15 was grey, trachyandesic, with 58 mass % SiO_2. After April 18, ash production decreased by one to two orders of magnitude. The composition was essentially the same, 57 % SiO_2, but the ash took on a more typical character, namely larger particles, black and glassy [2].

In addition to the VA, typical atmospheric aerosol particles, such as sodium nitrate (Fig. 3, ELPI 4, bands at 101, 185, 724, 1,068 (very strong, vs), and 1,385 cm^{-1}), titanium dioxide TiO_2 in the form of anatase (Fig. 3, ELPI 5, band at 145 cm^{-1}, vs), and soot (Fig. 3, ELPI 6), were found in the samples collected with ELPI. Furthermore, we found many particles with no distinguishable Raman bands, but intense fluorescence background. We assume that these particles consist of clay minerals, which are usually characterized by the lack of distinct Raman features, but strong fluorescence signals [19]. Due to significant differences between the spectra of typical atmospheric aerosol particles and VA, the latter were easily identified. Moreover, it is also possible to differentiate between VA and various particles of (micro)biological origin, e.g., pollen, bacteria, and their spores, which each exhibit specific Raman fingerprints [20, 21].

Figure 4 shows particles (VA-g 1–9) of the volcanic ash collected at the ground near the eruption of Eyjafjallajökull volcano and the corresponding Raman spectra. The particles are much larger (up to 200 μm) than the airborne VA particles (up to 50 μm), which is in accordance with the literature [2]. The particles are very angular and dark. The Raman spectra show the rather broad bands near 105, 160, 285, 470, 510 (vs), 660, and 1,000 cm^{-1} (Table 2), which suggest a disordered crystalline structure. Obviously, the spectral pattern of VA-g particles collected from the ground differs significantly from the spectra of airborne VA particles, indicating different chemical composition of these samples. As it was already mentioned, VA particles have size and age depending composition [4] that can explain the differences between the typically small (2–10 μm) airborne VA and big particles of the volcanic ash collected at the ground. Moreover, in contrast to VA-fp and VA-ap, which represent the particles from the eruption occurring on one or several days, VA-g ash can contain the particles from the entire eruption period (April/May 2010).

Fig. 4 Optical microscope images and corresponding Raman spectra of the volcanic ash particles VA-g, collected near at the ground near the eruption. The spectra were collected at the positions $x=0$, $y=0$

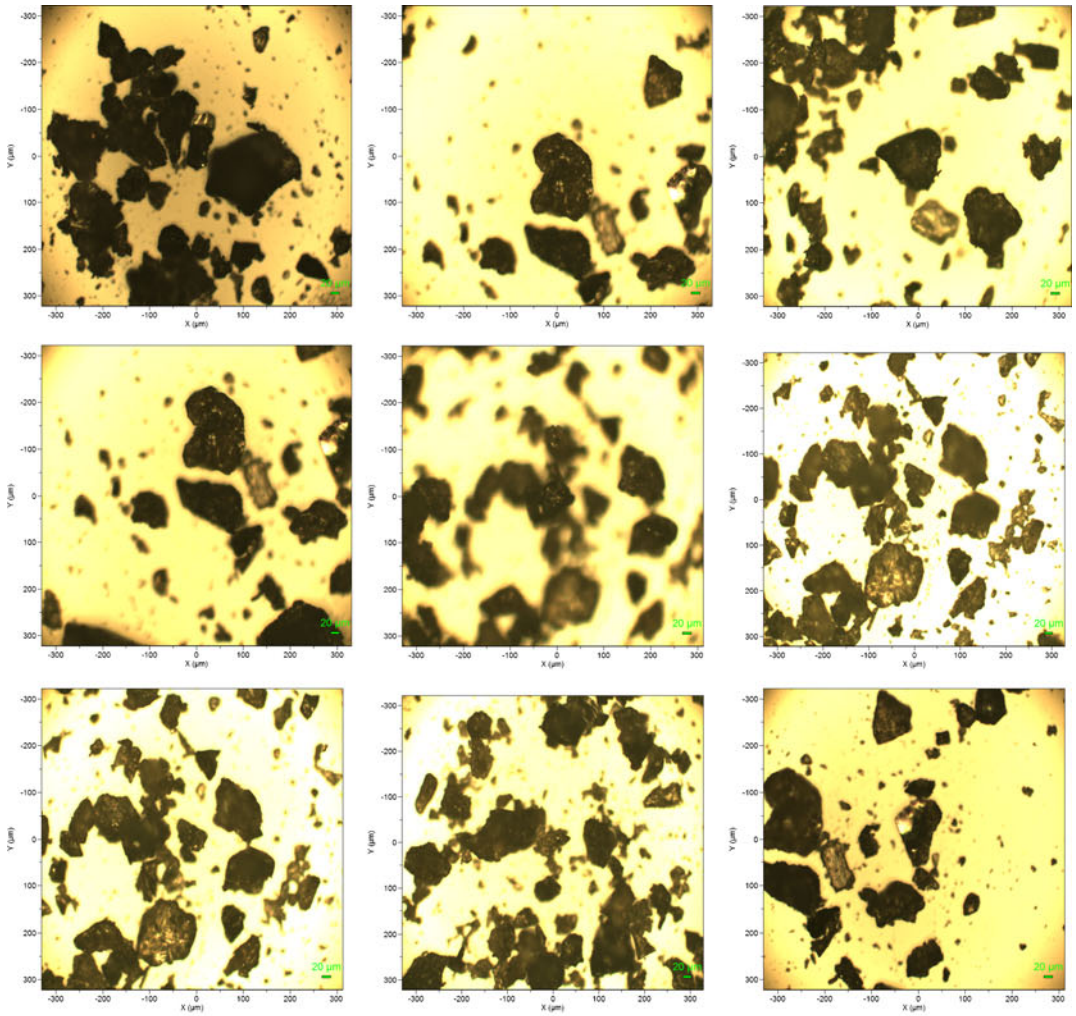

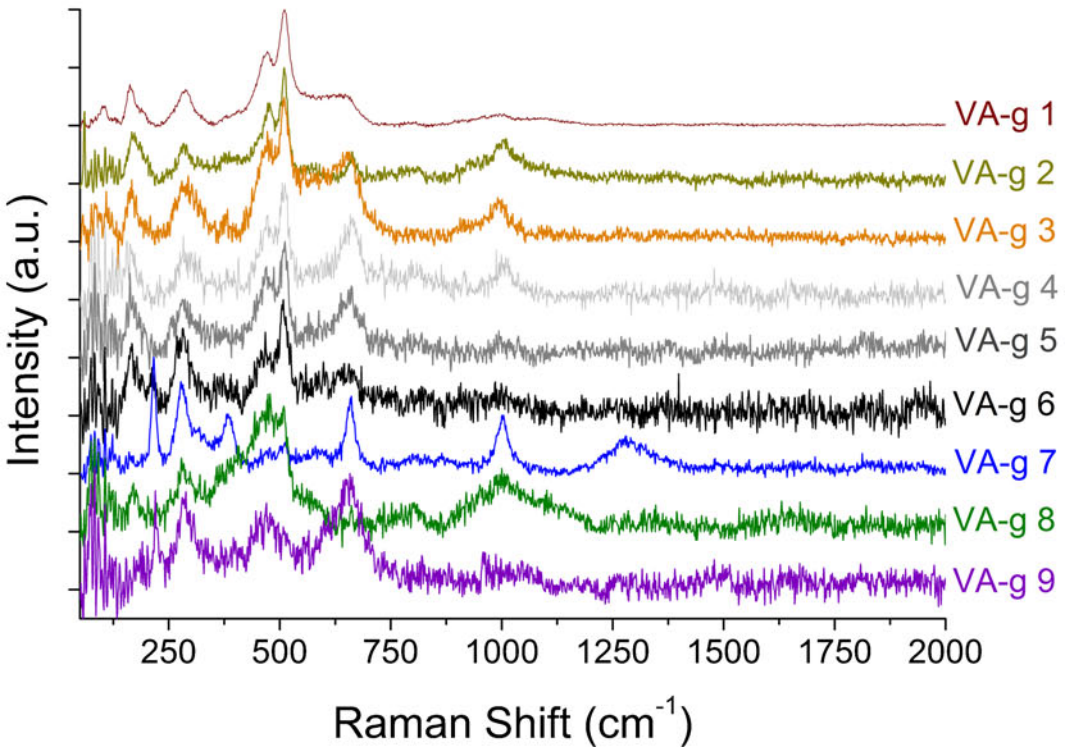
VA-g 1
VA-g 2
VA-g 3
VA-g 4
VA-g 5
VA-g 6
VA-g 7
VA-g 8
VA-g 9
Intensity (a.u.)
250
500
750
1000
1250
1500
1750
2000
Raman Shift (cm-1)

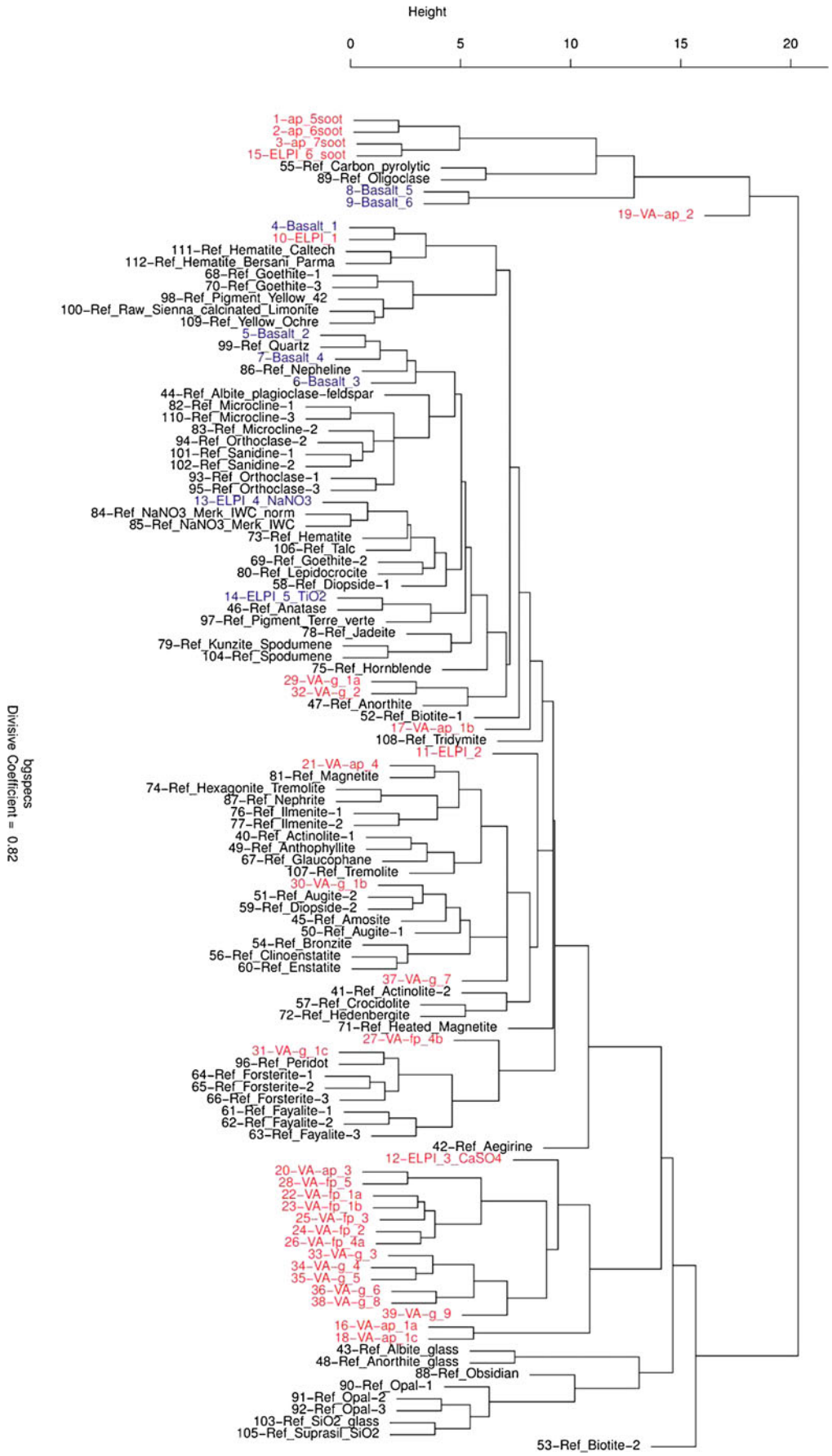
Height
0
5
10
15
20
bgspecs
Divisive Coefficient = 0.82
1-ap_5soot
2-ap_6soot
3-ap_7soot
15-ELPI_6_soot
55-Ref_Carbon_pyrolytic
89-Ref_Oligoclase
8-Basalt_5
9-Basalt_6
19-VA-ap_2
4-Basalt_1
10-ELPI_1
111-Ref_Hematite_Caltech
112-Ref_Hematite_Bersani_Parma
68-Ref_Goethite-1
70-Ref_Goethite-3
98-Ref_Pigment_Yellow_42
100-Ref_Raw_Sienna_calcinated_Limonite
109-Ref_Yellow_Ochre
5-Basalt_2
99-Ref_Quartz
7-Basalt_4
86-Ref_Nepheline
6-Basalt_3
44-Ref_Albite_plagioclase-feldspar
82-Ref_Microcline-1
110-Ref_Microcline-3
83-Ref_Microcline-2
94-Ref_Orthoclase-2
101-Ref_Sanidine-1
102-Ref_Sanidine-2
93-Ref_Orthoclase-1
95-Ref_Orthoclase-3
13-ELPI_4_NaNO3
84-Ref_NaNO3_Merk_IWC_norm
85-Ref_NaNO3_Merk_IWC
73-Ref_Hematite
106-Ref_Talc
69-Ref_Goethite-2
80-Ref_Lepidocrocite
58-Ref_Diopside-1
14-ELPI_5_TiO2
46-Ref_Anatase
97-Ref_Pigment_Terre_verte
78-Ref_Jadeite
79-Ref_Kunzite_Spodumene
104-Ref_Spodumene
75-Ref_Hornblende
29-VA-g_1a
32-VA-g_2
47-Ref_Anorthite
52-Ref_Biotite-1
17-VA-ap_1b
108-Ref_Tridymite
11-ELPI_2
21-VA-ap_4
81-Ref_Magnetite
74-Ref_Hexagonite_Tremolite
87-Ref_Nephrite
76-Ref_Ilmenite-1
77-Ref_Ilmenite-2
40-Ref_Actinolite-1
49-Ref_Anthophyllite
67-Ref_Glaucophane
107-Ref_Tremolite
30-VA-g_1b
51-Ref_Augite-2
59-Ref_Diopside-2
45-Ref_Amosite
50-Ref_Augite-1
54-Ref_Bronzite
56-Ref_Clinoenstatite
60-Ref_Enstatite
37-VA-g_7
41-Ref_Actinolite-2
57-Ref_Crocidolite
72-Ref_Hedenbergite
71-Ref_Heated_Magnetite
27-VA-fp_4b
31-VA-g_1c
96-Ref_Peridot
64-Ref_Forsterite-1
65-Ref_Forsterite-2
66-Ref_Forsterite-3
61-Ref_Fayalite-1
62-Ref_Fayalite-2
63-Ref_Fayalite-3
42-Ref_Aegirine
12-ELPI_3_CaSO4
20-VA-ap_3
28-VA-fp_5
22-VA-fp_1a
23-VA-fp_1b
25-VA-fp_3
24-VA-fp_2
26-VA-fp_4a
33-VA-g_3
34-VA-g_4
35-VA-g_5
36-VA-g_6
38-VA-g_8
39-VA-g_9
16-VA-ap_1a
18-VA-ap_1c
43-Ref_Albite_glass
48-Ref_Anorthite_glass
88-Ref_Obsidian
90-Ref_Opal-1
91-Ref_Opal-2
92-Ref_Opal-3
103-Ref_SiO2_glass
105-Ref_Suprasil_SiO2
53-Ref_Biotite-2

◀ **Fig. 5** Cluster tree for the sampled particles and reference spectra

Characterization of VA particles

In order to interpret the Raman spectra of volcanic particles, i.e., to characterize VA chemical composition and structure, the spectra from basaltic rock mineral as well as a wide range of reference spectra were taken into account. The choice of the distinct reference minerals or mineral groups (see "Experimental" section) was based on published data on the composition of VA from Eyjafjallajokull. Sigmundsson et al. [1] reported on an explosive summit eruption of trachyandesite beginning on April 14, 2010. This eruption was preceded by an effusive flank eruption of basalt from March 20 to April 12, 2010. Trachyandesite (or benmoreite) is an extrusive igneous rock which is dominated by alkali feldspar and sodic plagioclase along with one or more of the following mafic (magnesium and ferric) minerals: amphibole, biotite, or pyroxene. It contains little or no free quartz and sometimes small amounts of nepheline. Karlsdóttir et al. [3] pointed out that the eruption produced mainly trachyandesite, but became more silicic in May when trachyte was erupted. The latter consists of alkali feldspar, a low amount of plagioclase, and quartz or a feldspathoid (nepheline); clinopyroxene and olivine are common accessory minerals. Schumann et al. [4], who analyzed airborne VA by TEM and EDX, found that silicates and mixed particles are the most abundant groups for the particles larger than 500 nm. Most silicate grains (more than 90 %) are mixtures of various minerals, consisting predominantly of feldspars, amphiboles/pyroxenes, and pure SiO_2 minerals in variable proportions. We are not aware of any literature on RM analysis of chemical composition of VA from Eyjafjallajökull. RM study of other volcano samples taken at ground level, e.g., El Gasco pumice, western Spain [22] indicated the mineral composition is made of magnetite (Fe_3O_4), hematite (α-Fe_2O_3), and ilmenite ($FeTiO_3$). However, based on the chemical analysis of Eyjafjallajökull VA, where no [4] or a low amount (0.3–1.13 %) [2] of Ti was found, ilmenite cannot be expected in our samples. Furthermore, Laser Raman Spectroscopy has been applied for the characterization of Mount St. Helens (Washington) ash from the May 18, 1980. Here, besides three common crystallite silica polymorphs (i.e., quartz, cristobalite, and tridymite), Al_2O_3 and Fe_2O_3 have been identified [23–25]. Silica as well as Na Al silicate has been found by this method also in volcanic ash from Mt. Sakurajima in Japan from September 16 and October 2, 1981 [26]. As discussed in detail later, silica in airborne VA from Eyjafjallajökull is not crystallite, but rather amorphous.The cluster tree for the sampled particles and reference spectra is given in Fig. 5, and spectra for some groups including sampled particles are given in Figs. S8 to S17 in the ESM as reference. The cluster analysis and a priori knowledge from reference spectra allow an automatic discrimination of airborne particles into volcanic ash particles, soot particles, and other individual particles collected airborne. Also, the volcanic ash collected at ground surface is sorted into one distinct group, which is different from fresh and aged volcanic ash particles collected airborne. However, we did not find pronounced similarities of most of the glassy particles to basaltic rock or its mineral constituents. This makes sense, as the background correction removes the broad band (200–700 cm^{-1}) characteristic for the glassy matrices. While a detailed characterization of collected particles still requires manual intervention and database research (see below), the cluster analysis provides a rapid method to differentiate between particles origination from the volcano and other airborne particles and helps us to classify the particles according to its origin.

To get more information on chemical composition and structure of VA particles, we analyzed their spectra in detail and compared them with the spectra of reference compounds, chosen based on the CA results. As already mentioned, the VA particles collected from the fresh plumes (VA-fp 1–5) show quitesimilar spectra (see Fig. 1). Moreover, we found resemblances between the particles VA-fp 5 and VA-ap 3 from the fresh and aged plumes, respectively (Fig. 6).

The VA particles collected from the fresh plumes (VA-fp 1–5) show the spectra with characteristic very broad band, which extends from ca. 200 to ca. 700 cm^{-1}. This spectral signature is typical for glassy structures, i.e., SiO_2 glasses (Fig. 7, Table 2), alumosilicate (basaltic and rhyolitic) glasses [17], feldspar glasses (Fig. S18, ESM), as well as natural volcanic glasses [18]. The similarity of the broad band in the spectra of airborne VA particles and SiO_2 glasses suggests the presence of these amorphous compounds in glassy matrix of volcanic ash.

Schumann et al. [4] assumed that hematite is the main absorbing component in VA, since no phase information on the specific iron minerals which are present in the volcanic dust was available. We compared the Raman spectra of airborne VA-fp and VA-ap samples with reference ferric minerals (Figs. 6, 8 and Table 2) and found more similarities not to

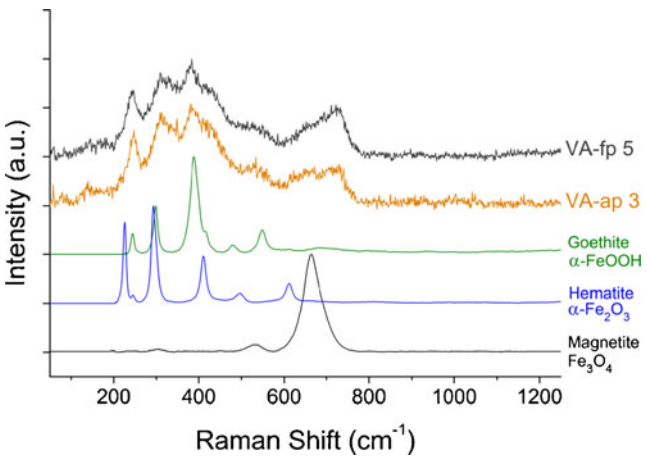

Fig. 6 Raman spectra of the airborne particles from the fresh and aged plumes (VA-fp 5 and VA-ap 3) as well as and reference ferric minerals

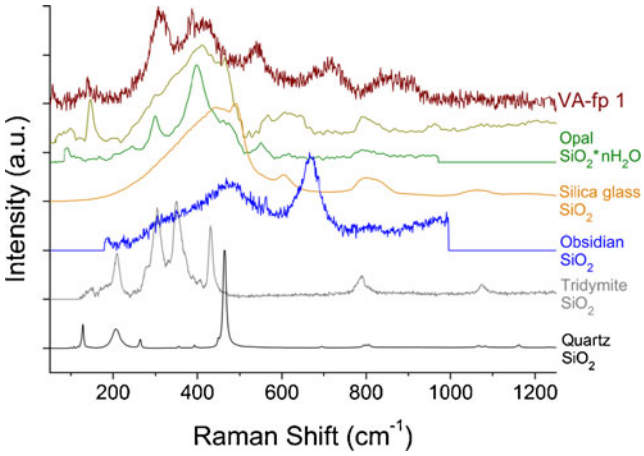

Fig. 7 Raman spectra of the airborne particle (VA-fp 1) and reference SiO_2 samples

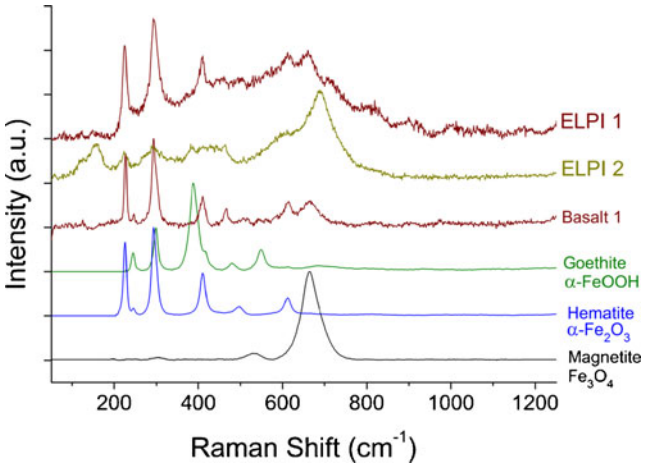

Fig. 9 Raman spectra of the aerosol particles (ELPI 1 and ELPI 2), basaltic rock (measurement point 1), and reference ferric minerals

hematite (α-Fe_2O_3), but rather to goethite (α-FeOOH). We did not observe the strong bands at 226 and 293 cm^{-1} typical for hematite [27–31], or the bands at 220 and 283 cm^{-1} which have been reported for hematite measured at high laser power [27, 30]. However, taken into account the broad band around 670 cm^{-1}, which is typical for all VA-fp and VA-ap, we cannot exclude the presence of heated/recrystallized hematite in our VA samples. A band at 671 cm^{-1} in the hematite spectrum has been described by Muralha et al. [31]. Some authors attribute it to the presence of a small proportion of magnetite in the hematite [31, 32]. A similar band has been reported by Leon et al. [33]: hematite rich clays show upshifted and broader peaks after being heated to temperatures above 800 °C. An additional broad peak at 680 cm^{-1} has been observed and attributed to recrystallization of hematite [33]. Furthermore, the authors have found that above the certain temperature (1,100 up to 1,250 °C, depending on the type of clay mineral), a new band appears in the region 730–750 cm^{-1}, while the Raman spectrum of hematite begins to disappear. This new band has been assigned to $8Al_2O_3{\cdot}SiO_2$ spinel [33]. This suggests that the broad band near 720 cm^{-1} in our VA-fp and VA-ap spectra could be attributed to spinel. The strongest band in VA-ap 4 spectrum at 670 cm^{-1} (Fig. S19, ESM) can be assigned to magnetite (and heated/recrystallized hematite).

In contrast to VA-fp and VA-ap, typical hematite bands were found in EPLI samples (ELPI 1 and ELPI 2, see below). Furthermore, as was expected, we did not observe the strong band of ilmenite ($FeTiO_3$) at 683 cm^{-1} (Fig. S19, ESM).

Basalt, which was mainly erupted by Eyjafjallajokull from March 20 to April 12, 2010 [1], is extrusive volcanic rock which contains less than 20 % quartz and less than 10 % feldspathoid and where at least 65 % of the feldspar is in the form of plagioclase. We analyzed basaltic rock and found very different spectral pattern (Fig. S20 and S21, ESM) from the different measurements spots on the sample, reflecting heterogeneous composition of this mineral. At the positions 2–4 and 5, we collected the spectra which were similar to quartz or feldspathoid nepheline $NaKAlSiO_4$ and plagioclase feldspar (oligoclase $(Na,Ca)(Al,Si)_4O_8$), respectively (Fig. S20, ESM). The positions 1 and 3 show the spectra which can be assigned

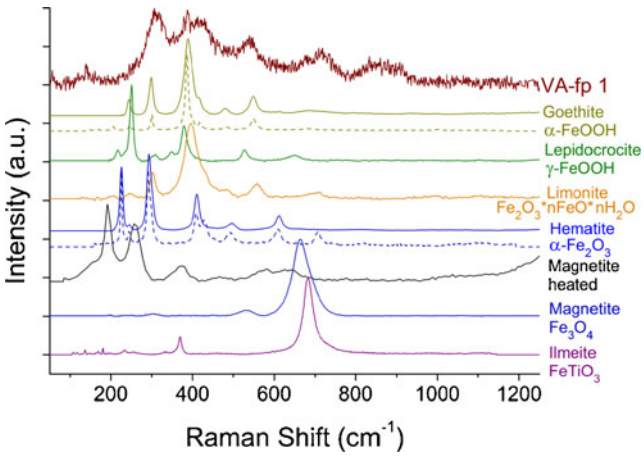

Fig. 8 Raman spectra of the airborne particle (VA-fp 1) and reference ferric minerals

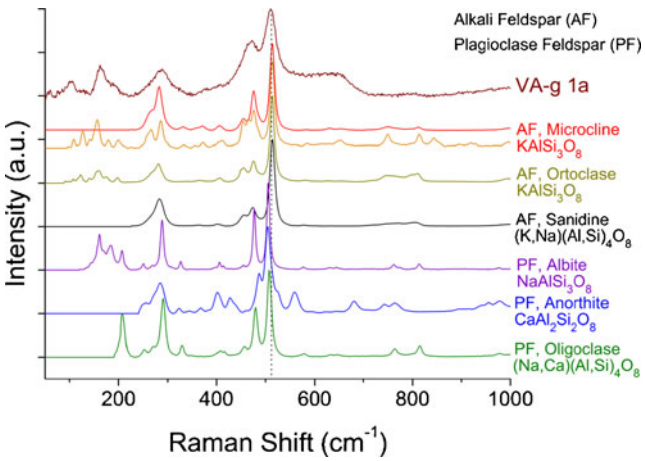

Fig. 10 Raman spectra of the ash particle VA-g and reference alkali and plagioclase feldspar samples

to hematite (Fig. S21, ESM). It is in good agreement with the results of CA (Fig. 5).

The comparison of the VA particles ELPI 1 and ELPI 2 with basaltic rock (spectrum Basalt 1, see Fig. 9, Table 2) suggests the predominance of such mineral (and hence hematite, see also Fig. 5) in these volcanic ash samples. The geological setting of the sampling location does not support the occurrence of basaltic rocks or basaltic particles from weathering as the Munich gravel plain is a glacial outwash plain composed of carbonates (limestone and dolomite) with traces of granite and gneiss.

The Raman spectra of VA-g 1–6 particles show characteristic spectral pattern with the strong band at 511 cm^{-1}, which is typical for feldspar minerals (Fig. 10 and Figs. S22, S23, ESM). Mernagh [34] has reported that alkali feldspars (series between $Na(Si_3Al)O_8$ and $K(Si_3Al)O_8$) show characteristic Raman band at 513 or 514 cm^{-1}, but for plagioclase feldspars (series between $Na(Si_3Al)O_8$ and $Ca(Si_2Al_2)O_8$) the band can be found between 500 and 510 cm^{-1}. So, we can assume the predominance of alkali feldspar minerals in VA-g samples. It is also in agreement with the reported eruption of trachyandesite and trachyte, which contains usually more alkali as plagioclase feldspars. However, taken into account the broadness of VA-g band at 511 cm^{-1} (490–535 cm^{-1}), we cannot completely exclude the presence of plagioclase feldspars in VA-g samples.

In contrast to the analyzed airborne VA, where similar spectra (or VA spectra with additional soot bands) (Figs. S2 and S4, ESM) were collected from the various parts of the particles, the VA sampled at the ground near the eruption often exhibits very different spectral pattern from the different measurements spots on the same particle. Fig. S23 (ESM) shows optical microscope image and corresponding spectra, which can be assigned to alkali feldspar, pyroxene, and nesosilicate (olivine) minerals, respectively.

Conclusion

We tested the feasibility of Raman microspectroscopy for the identification and characterization of VA airborne particles in terms of their mineral composition and crystalline and/or glassy structure. We found that RM is an efficient method for the discrimination of VA particles from other atmospheric particulate matter (e.g., soot, nitrates, sulfates, and clay minerals). Analysis of VA from fresh and aged plumes revealed a similar pattern in the Raman spectra, with characteristic bands below 1,000 cm^{-1}. Comparison of the spectra of airborne VA particles and of different ferric minerals indicated the predominance of goethite (α-FeOOH) for VA-fp and VA-ap and of hematite (α-Fe_2O_3) for ELPI samples. We assume a complex structure of airborne VA particles, where different crystalline mineral phases are embedded in glassy matrix (SiO_2 glasses). The differences observed in the spectra of aged and fresh particles suggest differences in their chemical composition and structure, which can be explained by varying proportions of different minerals, partial precipitation, and/or chemical aging of airborne VA particles during the transport. In order to get more information on the composition and structure of volcanic ash, we compared the spectra of VA particles with more than 40 glassy and crystalline minerals by applying the cluster analysis. The latter provides a rapid method to differentiate between particles originating from a volcano and other airborne particles, this enabling a faster assessment of ash clouds and their potential impact on air traffic. We believe that these results demonstrate a huge potential of RM for the fast and reliable analysis of airborne particles.

Acknowledgments The authors thank Michael Haisch for providing the volcanic ash particles sampled at ground near the eruption.

References

1. Sigmundsson F, Hreinsdottir S, Hooper A, Arnadottir T, Pedersen R, Roberts MJ, Oskarsson N, Auriac A, Decriem J, Einarsson P, Geirsson H, Hensch M, Ofeigsson BG, Sturkell E, Sveinbjoernsson H, Feigl KL (2010) Intrusion triggering of the 2010 Eyjafjallajoekull explosive eruption. Nature 468:426–430
2. Gislason SR, Hassenkam T, Nedel S, Bovet N, Eiriksdottir ES, Alfredsson HA, Hem CP, Balogh ZI, Dideriksen K, Oskarsson N, Sigfusson B, Larsen G, Stipp SLS (2011) Characterization of Eyjafjallajokull volcanic ash particles and a protocol for rapid risk assessment. Proc Natl Acad Sci U S A 108:7307–7312, S7307/7301-S7307/7303
3. Þorkelsson B, Karlsdóttir S, Gylfason ÁG, Höskuldsson Á, Brandsdóttir B, Ilyinskaya E, Gudmundsson MT, Högnadóttir Þ Report on the 2010 Eyjafjallaökull eruption, Island; Montreal, 13–15 June, 2012; pp 1–210, http://www.vedur.is/media/ICAOreport_web_lr.pdf
4. Schumann U, Weinzierl B, Reitebuch O, Schlager H, Minikin A, Forster C, Baumann R, Sailer T, Graf K, Mannstein H, Voigt C, Rahm S, Simmet R, Scheibe M, Lichtenstern M, Stock P, Rueba H, Schaeuble D, Tafferner A, Rautenhaus M, Gerz T, Ziereis H, Krautstrunk M, Mallaun C, Gayet JF, Lieke K, Kandler K, Ebert M, Weinbruch S, Stohl A, Gasteiger J, Gross S, Freudenthaler V, Wiegner M, Ansmann A, Tesche M, Olafsson H, Sturm K (2011) Airborne observations of the Eyjafjalla volcano ash cloud over Europe during air space closure in April and May 2010. Atmos Chem Phys 11:2245–2279
5. Weinzierl B, Sauer D, Minikin A, Reitebuch O, Dahlkötter F, Mayer B, Emde C, Tegen I, Gasteiger J, Petzold A, Veira A, Kueppers U, Schumann U (2012) On the visibility of airborne volcanic ash and mineral dust from the pilot's perspective in flight. J Phys Chem Earth 45–46:87–102
6. Gasteiger J, Gross S, Freudenthaler V, Wiegner M (2011) Volcanic ash from Iceland over Munich: mass concentration retrieved from ground-based remote sensing measurements. Atmos Chem Phys 11: 2209–2223
7. Schäfer K, Thomas W, Peters A, Ries L, Obleitner F, Schnelle-Kreis J, Birmili W, Diemer J, Fricke W, Junkermann W, Pitz M, Emeis S, Forkel R, Suppan P, Flentje H, Gilge S, Wichmann HE, Meinhardt F, Zimmermann R, Weinhold K, Soentgen J, Münkel C, Freuer C, Cyrys J (2011) Influences of the 2010 Eyjafjallajoekull volcanic

plume on air quality in the northern Alpine region. Atmos Chem Phys 11:8555–8575
8. Weber K, Eliasson J, Vogel A, Fischer C, Pohl T, van Haren G, Meier M, Grobety B, Dahmann D (2012) Airborne in-situ investigations of the Eyjafjallajoekull volcanic ash plume on Iceland and over north-western Germany with light aircrafts and optical particle counters. Atmos Environ 48:9–21
9. McCreery RL (2000) Raman spectroscopy for chemical analysis. Wiley, New York, pp 15–35
10. Ivleva NP, McKeon U, Niessner R, Pöschl U (2007) Raman microspectroscopic analysis of size-resolved atmospheric aerosol particle samples collected with an ELPI: soot, humic-like substances, and inorganic compounds. Aerosol Sci Technol 41:655–671
11. Casadevall TJ Volcanic hazards and aviation safety: lessons of the past decade, Flight Safety Foundation–Flight Safety Digest; May, 1993; pp 1–9, http://www.caa.co.uk/docs/375/fsd_may93_p1-9.pdf
12. R Core Team (2012) R: A language and environment for statistical computing. R Foundation for Statistical Computing, Vienna. http://www.R-Project.org/
13. Morhac M, Kliman J, Matousek V, Veselsky M, Turzo I (1997) Efficient one- and two-dimensional gold deconvolution and its application to gamma-ray spectra decomposition. Nucl Instrum Methods Phys Res, Sect A 401:385–408
14. Morhac M, Kliman J, Matousek V, Veselsky M, Turzo I (1997) Background elimination methods for multidimensional coincidence gamma-ray spectra. Nucl Instrum Methods Phys Res, Sect A 401: 113–132
15. Morhac M, Kliman J, Matousek V, Veselsky M, Turzo I (2000) Identification of peaks in multidimensional coincidence gamma-ray spectra. Nucl Instrum Methods Phys Res, Sect A 443:108–125
16. Kaufman L, Rousseeuw PJ (1990) Finding groups in data. An introduction to cluster analysis. Wiley, New York
17. Lin C-C, L-g L (2006) Composition dependence of elasticity in aluminosilicate glasses. Phys Chem Miner 33:332–346
18. Zotov N (2003) Structure of natural volcanic glasses: diffraction versus spectroscopic perspective. J Non-Cryst Solids 323:1–6
19. Sobanska S, Hwang H, Choel M, Jung H-J, Eom H-J, Kim H, Barbillat J, Ro C-U (2012) Investigation of the chemical mixing state of individual Asian dust particles by the combined use of electron probe X-ray microanalysis and Raman microspectrometry. Anal Chem 84:3145–3154
20. Ivleva NP, Niessner R, Panne U (2005) Characterization and discrimination of pollen by Raman microscopy. Anal Bioanal Chem 381: 261–267
21. Rösch P, Harz M, Schmitt M, Peschke K-D, Ronneberger O, Burkhardt H, Motzkus H-W, Lankers M, Hofer S, Thiele H, Popp J (2005) Chemotaxonomic identification of single bacteria by micro-Raman spectroscopy: application to clean-room-relevant biological contaminations. Appl Environ Microbiol 71:1626–1637
22. Rull F, Martinez-Frias J, Rodriguez-Losada JA (2007) Micro-Raman spectroscopic study of El Gasco pumice, western Spain. J Raman Spectrosc 38:239–244
23. Farwell SO, Gage DR (1981) Crystalline silica in Mount St. Helens ash. Anal Chem 53:1529A-1530A, 1532A
24. Gage DR, Farwell SO (1981) Laser Raman spectrometry for the determination of crystalline silica polymorphs in volcanic ash. Anal Chem 53:2123–2127
25. Ishizaki H, Tu AT (1982) Laser Raman spectroscopic analysis of Mount St. Helens [Washington] ash from the May 18, 1980 eruption. J Environ Sci 25:32–33
26. Ishizaki H, Tu AT (1982) Laser Raman spectroscopic analysis of volcanic ash from Mt. Sakurajima in Japan. Appl Spectrosc 36:587–588
27. de Faria DLA, Silva SV, de Oliveira MT (1997) Raman microspectroscopy of some iron oxides and oxyhydroxides. J Raman Spectrosc 28:873–878
28. Popp J, Tarcea N, Kiefer W, Hilchenbach M, Thomas N, Stuffler T, Hofer S, Stoffler D, Greshake A (2002) The effect of surface texture on the mineralogical analysis of chondritic meteorites using Raman spectroscopy. Planet Space Sci 50:865–870
29. Edwards HGM, Farwell DW, De Faria DLA, Monteiro AMF, Afonso MC, De Blasis P, Eggers S (2001) Raman spectroscopic study of 3000-year-old human skeletal remains from a sambaqui, Santa Catarina, Brazil. J Raman Spectrosc 32:17–22
30. Bersani D, Lottici PP, Montenero A (1999) Micro-Raman investigation of iron oxide films and powders produced by sol–gel syntheses. J Raman Spectrosc 30:355–360
31. Muralha VSF, Rehren T, Clark RJH (2011) Characterization of an iron smelting slag from Zimbabwe by Raman microscopy and electron beam analysis. J Raman Spectrosc 42:2077–2084
32. van der Weerd J, Rehren T, Firth S, Clark RJH (2004) Identification of iron oxide impurities in earliest industrial-scale processed platinum. Mater Charact 53:63–70
33. Leon Y, Lofrumento C, Zoppi A, Carles R, Castellucci EM, Sciau P (2010) Micro-Raman investigation of terra sigillata slips: a comparative study of central Italian and southern Gaul productions. J Raman Spectrosc 41:1260–1265
34. Mernagh TP (1991) Use of the laser Raman microprobe for discrimination amongst feldspar minerals. J Raman Spectrosc 22:453–457